FOREX Publication
Open Access | Rapid and quality publishing

International Journal of
Electrical and Electronics Research (IJEER)
Research Article | Volume 14, Issue 1| Pages 110-122 |e-ISSN: 2347-470X

An Enhanced Loss Model–Based Online Flux Optimization Technique for Vector-Controlled Induction Motor Drives Including Leakage Inductance

B Hima Deepthi[1], P Srinivasa Varma[1], M Kiran Kumar[1], K V Govardhan Rao[2*]
[1]*Department of Electrical and Electronics Engineering, Koneru Lakshmaiah Education Foundation, Vaddeswaram, A.P, India*
[2]*Department of Electrical and Electronics Engineering, St. Martin's Engineering College, Secunderabad, Telangana, India*

***Correspondence:** *K V Govardhan Rao*; *kv.govardhanrao@gmail.com*

ABSTRACT- A fresh and original approach is presented in this research as a means of controlling the amount of flux that is produced by an induction motor drive. Some of the algorithms that are used to decrease losses in induction motors include a loss-model based technique, which is one of several algorithms. Two advantages of this technique are its quick response and accurate conclusions. On the other hand, precise motor drive and loss modelling is necessary for the success of this strategy. During the process of developing the loss model, one of the ongoing challenges is to achieve accuracy while simultaneously controlling complexity. In the present work, an improved controlling approach is proposed for the purpose of determining the optimal flux level for a vector-controlled induction motor in order to achieve the highest possible efficiency of the drive. In a *dq* model of an Induction Motor (IM), the rotor magnetizing current serves as a reference point for the model. After this transformation eliminates any rotor-side leakage inductance, we are able to derive the motor loss model by making use of the *dq* components that are included in the steady-state motor model. The problem of leaking inductances is not ignored by the new method, despite the fact that it is a straightforward application.

Keywords: Induction Motor, Loss Minimization, Stator Flux, Rotor Flux, Loss Calculation, Torque Control.

ARTICLE INFORMATION
Author(s): B Hima Deepthi, P Srinivasa Varma, M Kiran Kumar, K V Govardhan Rao;
Received: 09/09/2025; **Accepted**: 12/01/2026; **Published**: 10/03/2026;
E- ISSN: 2347-470X;
Paper Id: IJEER0909A12;
Citation: 10.37391/ijeer.140112
Webpage-link:
https://ijeer.forexjournal.co.in/archive/volume-14/ijeer-140112.html

Publisher's Note: FOREX Publication stays neutral with regard to jurisdictional claims in Published maps and institutional affiliations.

1. INTRODUCTION

Motors consume more than 50% of all electrical energy, and induction motors are a common choice for electrical drives because of their low cost, long lifespan, and reliable performance. Transmission loss, motor loss, grid loss, and converter loss are all components of electrical motor driving losses. There have been developments in materials, designs, and construction methods aimed at increasing efficiency [1]. Still, control tactics have a big impact on converter and motor efficiency, especially at low loads.

An induction motor with a three-phase wound rotor and a hybrid speed-control mechanism is introduced. Combining FOC with traditional controllers, the suggested method uses vector control. By integrating FOC with traditional controller features, this approach enhances the three-phase induction motor's speed response. Using simulation results and the implementation of proportional integral - field oriented control (PI-FOC), the performance of the hybrid system controller is analysed [2]. This study develops and tests the V/f scalar control for induction motor drives that are fed by 3ϕ wavelet modulated DC-AC power electronic converters. J and γ are the typical properties of the wavelet modulation method, which is determined by the highest level of resolution. The output voltage magnitude of a three-phase wavelet modulated inverter is determined by J, and γ relates the number of switching pulses to the output voltage half cycle.

By modulating these two parameters of the wavelet modulation approach, it is possible to get V/f scalar control of induction motor drives. By testing its functionality under different operating situations with IM Drives, we can determine the V/f scalar control of a wavelet-modulated DC-AC PEC [3]. The article delves into the specifics of building and implementing an NN-based CS flaws classifier. The suggested technique employs a multilayer perceptron (MLP) architecture that is derived from individual samples of the stator phase current data. In order to build NN input vectors free of limitations caused by changes in the machine's operating state (load, rotational speed), the tests show methods that accomplish this. Furthermore, by employing harmonic analysis, it is possible to optimise the network's input vector with respect to the reviewed damages. This article demonstrates how diagnostic systems applied to physical objects can make complete use of the mathematical model [4].

The article suggests a duty cycle method for predictive control using an optimised control set model. To begin, we build a brand-new 24 VVC control set that is virtual.

Owing to a combination with duty cycle modulation techniques, the new set of controls takes use of multi-directional, evenly

FOREX Publication
Open Access | Rapid and quality publishing
International Journal of Electrical and Electronics Research (IJEER)
Research Article | Volume 14, Issue 1| Pages 110-122 |e-ISSN: 2347-470X

distributed voltage vectors. Increasing the number of potential vectors in the new control system allows for more precise control. Furthermore, the system proposes an error-minimizing method for duty cycle calculations that simultaneously considers the currents along the *dq*-axis, even in the case of a single active voltage vector [5]. The effective approach is called ETV-SMPC, which stands for two-vector-based sequential model predictive control. An efficient method for SMPC with an expanded control set is the intended outcome. We offer a quick method for selecting candidates from the collection in order to come up with workable combinations. By eliminating many unnecessary candidates, the suggested strategy lowers the computational cost. In order to improve the evaluation performance compared to traditional designs, the cost functions for assessing torque and flux mistakes are designed in various forms, made possible by the flexible sequential evaluation structure [6], because of its straightforward design and ease of implementation, Intermittent field-oriented control (IFOC) drives for induction motors have found widespread application. In IFOC, the rotor time constant is the most important factor. But rotor inductance fluctuates with real-world magnitude, while rotor resistance increases with temperature. On top of that, it is difficult to get a good estimate of these parameters. When the estimated and actual rotor time constants are not in perfect agreement, the IFOC vector control performance suffers. This is due to the imperfect estimation of the rotor flux position.

The traditional Q-MRAS method is commonly employed to correct for the rotor time constant, and this work offers a theoretical examination of the implications of inductance faults in this method [7]. Motor drives with two-level voltage source inverters can benefit from the low-computational-burden model predictive flux control (MPFC) that uses DSVM and optimal switching sequence (OSS) to optimise switching frequency (SF) and computational burden. The DSVM extends MPFC prediction candidates and considerably improves controller performance [8]. In this article, we take a look at the current control tactics for induction motors (IMs) and assess their effectiveness using vector-controlled (VC-) techniques. Both scalar control and variable-speed drive control have been the subject of much study. IM drive closed and open loops describe the speed and V/f control of SCC-based systems.

The functions, advantages, and disadvantages of both direct and indirect field-oriented control systems are displayed. It also takes a look at the IM direct torque control (DTC) method. Many VC approaches are covered and investigated, including microprocessor/digital control, model reference adaptive control (MRAC), sliding mode control (SMC), intelligent control fuzzy logic (FL), and artificial neural networks (ANNs), after carefully selecting and systematising literature sources, this report presents a comprehensive investigation and criterion analysis of induction motor drive energy efficiency enhancement. Five major and 48 minor study areas exist in this discipline.

The results indicate that scientific results adaption and their effective and widespread applications[4]. An efficiency optimisation approach for vector-controlled Induction Motor (IM) Drives and analyses their performance under various operating situations. Optimal control of direct axis stator current, which regulates rotor flux, minimises IM Drive's controllable electrical loss. Thus, lowering the rotor flux decreases core losses and optimises motor efficiency. A fuzzy logic-based fault diagnostic technique is presented and tested for diagnosing various open-circuit (OC) faults in a unique dual-winding fault-tolerant permanent magnet motor (DFPMM) drive. With fewer separate power supplies and switches, the suggested DFPMM drive outperforms multi-phase fault-tolerant drives in terms of power density, utilisation, and reliability. The study details and proves experimentally an improved Integral Sliding Mode Control (ISMC) for mechanical speed of Induction Motors (IMs).

Indirect Field Oriented Control and *dq* synchronous reference frame were used to build the proposed controller. An upgraded ISMC surface guarantees global asymptotic speed tracking with model errors and load torque changes [9]. The multi-phase motors are more reliable and perform better than three-phase ones for electrified transportation (Transportation) systems, but their optimal design and control are more difficult. This article introduces a high-reliability electric drive system for auxiliary systems in Transportation using dual three-phase permanent magnet synchronous motors (DTP PMSM) [10].

In terms of control approach, there are primarily two ways to increase motor efficiency:
1. Try to locate a search controller (SC) and
2. Find a controller that is based on a loss model (LMC).

By monitoring the input power, the search controller is able to minimize it for a given torque and speed by constantly seeking the ideal flux level or associated variables. Torque ripples and the search controller's sluggish convergence are two major drawbacks [11]. The model-based controller determines the optimal flux level to minimize losses by utilizing the machine model [12], [13]. Operating smoothly and without torque fluctuations is guaranteed by LMC's excellent efficiency. Nevertheless, the accuracy is dependent upon the motor drive and losses being accurately modelled [14]. The optimal flux level expression in their model [15], [16] is structured differently from the one in, albeit this is an important point to remember [17], [18]. As a result, that phrase cannot be used as a general model for different kinds of motors.

Perfect would be a loss model that is both easy to understand and accurate. This study presents an induction motor model that takes the rotor magnetizing current into account and features an iron loss resistor [19], [20]. Since this is the case, the rotor side leakage inductance is ignored. In the same way as the one given in, we can use this model to construct the equation that determines the optimal flux level [21], [22]. When developing the LMA, this method is frequently used to account for the leakage inductance [23]. Equally consistent with earlier efforts is the structure of the optimal flux equation. It can be easily included into current loss minimization techniques by changing the motor parameters in relation to the magnetizing current [24]. We use simulation to test how well the proposed controller works [25]. According to the findings, compared to not

FOREX Publication
Open Access | Rapid and quality publishing
International Journal of Electrical and Electronics Research (IJEER)
Research Article | Volume 14, Issue 1| Pages 110-122 |e-ISSN: 2347-470X

employing the LMA, the recommended model improves the drive's performance by reducing torque variations and increasing power efficiency[20], [26], [27].

1.1. Research Gap and Contributions

Extensive research has been reported on efficiency optimization of induction motor drives using search controllers (SC) and loss model–based controllers (LMC). Search controller–based approaches minimize input power by continuously perturbing the flux or current reference; however, these methods are characterized by slow convergence, steady-state oscillations, and noticeable torque ripple, particularly under light-load conditions. Loss model–based controllers overcome these limitations by directly computing the optimal flux level, but their effectiveness strongly depends on the accuracy of the motor loss model. Many existing LMC approaches either neglect iron losses, ignore leakage inductance, or assume simplified motor models that limit their applicability across a wide operating range.

Furthermore, several reported studies focus on loss minimization at a single operating point or under nominal conditions, without validating robustness against parameter variations or different speed–load combinations. The lack of explicit treatment of leakage inductance and iron loss effects in the optimal flux derivation remains a key limitation in much of the existing literature.

The proposed work addresses these gaps by developing an enhanced loss model that incorporates both iron losses through an equivalent resistance and leakage inductance effects within a rotor magnetizing current–oriented *dq* reference frame. Unlike conventional LMC methods, the proposed approach maintains analytical simplicity while providing improved physical accuracy, enabling fast and smooth loss minimization without iterative search or torque oscillations. Additionally, the proposed strategy is validated under multiple operating conditions and parameter variations, demonstrating robustness and practical relevance. These features clearly differentiate the proposed method from existing SC and LMC approaches and establish its contribution to efficient vector-controlled induction motor drives.

In this work, an advanced control technique to optimize the flux level and efficiency for vector-controlled induction motor drive is proposed. Addressing loss minimisation with or without leakage inductance is the focus of the suggested methodology. Following the introduction and literature review in *section 1*, *section 2* presents the results of the loss model analysis for the induction motor. The approach of minimising the induction motor loss model is detailed in *section 3*. *Section 4* provides a discussion of the outcomes. *Section 5* concludes the entire thing.

2. LOSS MODEL ANALYSIS OF INDUCTION MOTOR

2.1. Definition and Role of Leakage Inductances

In an induction motor, the total stator and rotor inductances consist of magnetizing and leakage components. The stator inductance L_s and rotor inductance L_r are expressed as

$$L_s = L_{ls} + L_m, L_r = L_{lr} + L_m$$

where $L_{ls}$and L_{lr}denote the stator and rotor leakage inductances, respectively, and $L_m$is the magnetizing inductance. The leakage inductances represent the portions of the stator and rotor flux that do not contribute to the mutual air-gap flux linking both windings.

Physically, the stator leakage inductance L_{ls} accounts for the flux confined to the stator slots and end windings, which primarily affects the stator voltage drop and transient current dynamics. Similarly, the rotor leakage inductance L_{lr} represents flux that links only the rotor conductors, influencing rotor current distribution and torque production. These leakage flux components do not participate in energy conversion but contribute to additional copper losses and alter the effective flux linkage of the machine.

In the proposed rotor magnetizing current–oriented reference frame, the *d*-axis is aligned with the magnetizing current, allowing a clear separation between flux-producing and torque-producing current components. Under steady-state conditions, the effect of leakage inductances is reflected through their influence on the equivalent inductance seen by the stator and rotor circuits. For analytical clarity, the loss model is formulated considering both cases: *(i)* neglecting rotor-side leakage inductance to obtain a simplified optimal flux expression, and *(ii)* retaining leakage inductance terms to evaluate their impact on current dynamics, loss distribution, and efficiency optimization.

By explicitly defining and incorporating leakage inductances into the *dq* axis voltage and flux equations, the revised formulation ensures that their influence on flux linkage, current dynamics, and loss minimization is accurately represented.

Changing the flux linkage constants modifies the IM equivalent circuit. The rotor flux is defined as $\Psi_r = L_m i_{mr}$. this investigation makes use of a circuit analogous to that which is associated with the current that magnetises the rotor. The rationale for this modification is illustrated in *figure 1*.

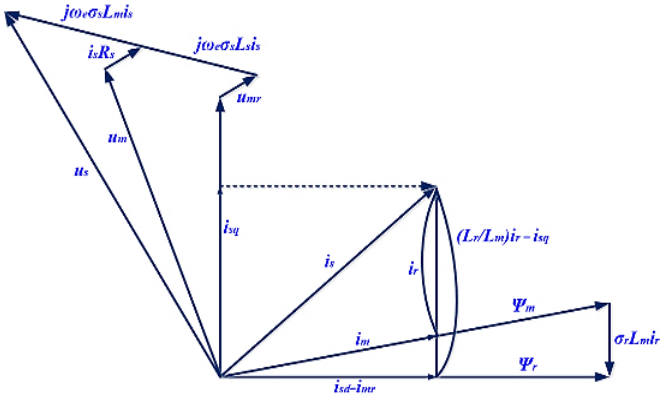

Figure. 1 Induction Motor Phasor Diagram for the Steady-State Circuit

In a reference frame that is fixed to the rotor's magnetizing current, a resistor R_f', is connected in parallel to the magnetizing

FOREX Publication
Open Access | Rapid and quality publishing
International Journal of Electrical and Electronics Research (IJEER)
Research Article | Volume 14, Issue 1| Pages 110-122 |e-ISSN: 2347-470X

inductance to account for iron loss. The way of the magnetizing current i_{mr} has been aligned with the d-axis, as seen in *figures 2* and *3*. The space vector motor model is identified by the differential operator $p \equiv d/dt$ while the reference frame is rotating. The electrical rotor speed and the electrical angular speed $\omega_e = d\theta_e/dt$ of the rotor flux $\omega_r = d\theta_r/dt$ are both included in this model.

$$v_s = R_s i_s + pL'_s i_s + j\omega_e L'_s i_s + pL'_m i_m + j\omega_e L'_m i_m \quad (1)$$

$$i_s = i_m + i_f + i_r$$

$$i_s = i_m + (p + j\omega_e)\frac{L'_m}{R'_f} i_m + \left(p + j(\omega_e - \omega_r)\right)\frac{L'_m}{R'_f} i_m \quad (2)$$

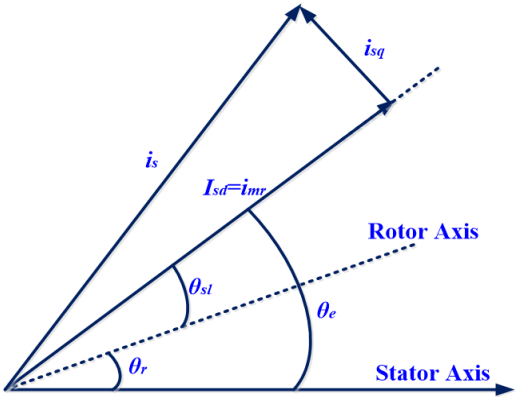

Figure. 2 A phasor diagram showing the induction motor's stat and rotor axes

2.2. Iron-Loss Representation in the Proposed Model

In induction motor loss analysis, iron losses mainly consist of hysteresis and eddy current losses, both of which are strongly dependent on the air-gap flux level and operating frequency. For steady-state operation under sinusoidal excitation, these losses can be effectively represented by an equivalent iron-loss resistance R_{fe}connected in parallel with the magnetizing inductance L_m. This modelling approach provides a lumped representation of core losses while preserving the physical relationship between magnetizing flux and power dissipation in the iron core.

The use of a single equivalent iron-loss resistor is a well-established and widely adopted practice in efficiency optimization studies of vector-controlled induction motor drives, particularly when real-time control implementation and analytical tractability are required. By incorporating R_{fe}in parallel with L_m, the iron loss current component is explicitly separated from the torque-producing and flux-producing currents, enabling a clear analytical formulation of total losses in the *dq* reference frame.

Although this approach does not explicitly separate hysteresis and eddy current losses or account for saturation-dependent and frequency-varying effects, it provides sufficient accuracy within the normal operating flux and frequency range considered in this study. The primary objective of the proposed model is loss minimization and efficiency optimization rather than detailed electromagnetic loss decomposition. Therefore, the single-resistor iron-loss model offers an effective compromise between physical fidelity and computational simplicity, making it suitable for online loss minimization control schemes.

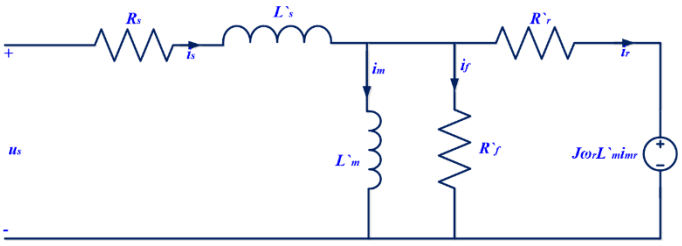

Using $v_s = v_{sd} + jv_{sq}$
$i_s = i_{sd} + ji_{sq}$
$i_m = i_{md} + ji_{mq}$
$i_{mq} = 0$
$i_{md} = i_{mr} = Constant$, for the control scheme of rotor-flux-orientation we will obtain *eq. (1)-(2).*

$$v_{sd} = R_s i_{sd} + pL'_s i_{sd} - \omega_e L'_s i_{sq} + pL'_m i_{mr} \quad (3)$$

$$v_{sq} = R_s i_{sq} + pL'_s i_{sq} - \omega_e L'_s i_{sd} + pL'_m i_{mr} \quad (4)$$

$$i_{sd} = i_{mr} + p\left(\frac{L'_m}{R'_f} + \frac{L'_m}{R'_r}\right) i_{mr} \quad (5)$$

$$i_{sq} = \omega_e \frac{L'_m}{R'_f} i_{mr} + (\omega_e - \omega_r)\frac{L'_m}{R'_r} i_{mr} \quad (6)$$

Let $R_t = R'_r \parallel R'_f$, *eq. (3)* magnetizing current can be expressed as,

$$i_{mr} = \frac{1}{1+p\left(\frac{L'_m}{R'_f}+\frac{L'_m}{R'_r}\right)} i_{sd} = \frac{1}{1+p\frac{L'_m}{R_t}} i_{sd} \quad (7)$$

From *eq. (6)*, The slip speed can be expressed as,

$$\omega_{slip} = \frac{R'_r}{L'_m}\frac{i_{sq}}{i_{mr}} - \omega_e \frac{R'_r}{R'_f} = \frac{R_t}{L'_m}\frac{i_{sq}}{i_{mr}} - \omega_r \frac{R_t}{R'_f} \quad (8)$$

When analysing not to overlook the absence of leakage inductance which is present on rotor side when examining this motor model in its steady state. As an added bonus, the total of the re-calculated rotor current i_r and the iron current i_f is perpendicular to the magnetizing current i_{mr}. This circuit shows how the stator current, denoted as i_s, is broken down into the flux generator and torque regulator, denoted as $i_{sd} = i_{mr}$. Keep in mind that the torque can be adjusted. *Figures 4* and *5* demonstrate the field-oriented representation of the steady-state IM equivalent circuit, which is derived from the motor model *eq. (3)-(6)*. The terms involving differentiation become zero in steady-state, therefore equations v_{sd} *and* i_{sd} may be used to get *figure 4*, while equations v_{sq} *and* i_{sq} can be used to generate *figure 5*, respectively.

FOREX Publication
Open Access | Rapid and quality publishing
International Journal of Electrical and Electronics Research (IJEER)
Research Article | Volume 14, Issue 1| Pages 110-122 |e-ISSN: 2347-470X

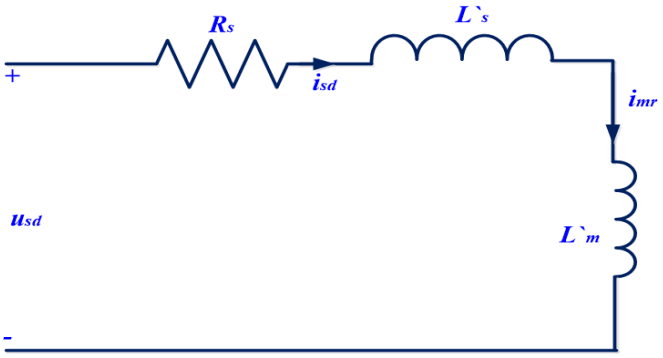

Figure 4. Steady State Induction Motor circuit of *d*-axis

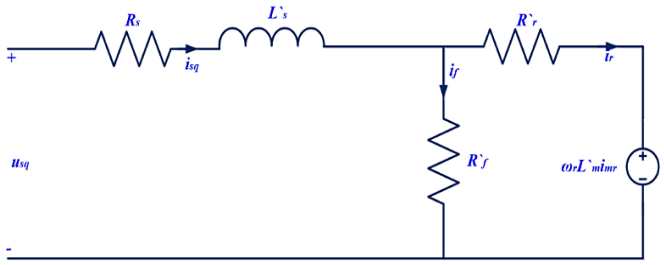

Figure 5. Steady State Induction Motor circuit of *q*-axis

3. LOSS MODEL MINIMIZATION STRATEGY FOR AN INDUCTION MOTOR

Previously conducted studies often used a method that ignored the impact of leakage inductance. The loss model can be derived more easily using the decay characteristic of the suggested motor typical, which removes the requirement to assume that the model is simple. Instead of stray, friction, windage or converter losses, stator and rotor copper and iron losses are the main culprits in total power loss. These days things like windage, stray and friction are all also considered.

$$P_{total} = P_{stator\ copper\ losses} + P_{iron\ losses} + P_{rotor\ copper\ losses}$$

$$P_{total} = R_s\left(i_{sd}^2 + i_{sq}^2\right) + R_f'\left(i_{sq} - i_r\right)^2 + R_r' i_r^2 \qquad (9)$$

Because there are no other real-state variables other than the stator voltage and current, we must express the entire losses as i_{sd} *and* i_{sq}.

From *figure 4*, Rotor current speed is

$$i_r = i_{sq} - i_f = i_{sq} - \frac{R_r'}{R_f'} i_r - \omega_r \frac{L_m'}{R_f'} i_{sd} \qquad (10)$$

Then,

$$i_r = \frac{R_f'}{R_f' + R_r'} i_{sq} - \omega_r \frac{L_m'}{R_f' + R_r'} i_{sd} \qquad (11)$$

Substitute *eq. (11)* into *eq. (9)* Therefore,

$$P_{total} = R_d i_{sd}^2 + R_q i_{sq}^2 \qquad (12)$$

Where,

$$R_d = R_s + \frac{L_m'^2}{R_f' + R_r'} \omega_r^2 \quad \text{and} \quad R_q = R_s + \frac{R_f' R_r'}{R_f' + R_r'}$$

The developed torque can be expressed as, from *fig. (4)* and *eq. (11)*, then the torque can be expressed as

$$T_e = \frac{3}{2} Z_p L_m' i_{mr} i_r$$

$$T_e = \frac{3}{2} Z_p L_m' \left(\frac{R_f'}{R_f' + R_r'}\right) i_{sq} i_{mr} - \frac{3}{2} Z_p \frac{\left(L_m' i_{mr}\right)^2}{R_f' + R_r'} \omega_r \qquad (13)$$

This torque can be rewritten like, with the help of *eq. (8)*,

$$T_e = \frac{3}{2} Z_p \frac{\left(L_m' i_{mr}\right)^2}{R_r'} \omega_{slip}$$

$$T_e = \frac{3}{2} Z_p L_m' i_{sq} i_{mr} - \frac{3}{2} Z_p \frac{\left(L_m' i_{mr}\right)^2}{R_f'} \omega_e \qquad (14)$$

The second term on the right side of the expression of *eq. (8)* is used in *eq. (14)*, the torque expression *eq. (14)* becomes same as *eq. (12)*, then accounts for the developed torque caused by the resistance from iron loss.

$$\left(R_f' + R_r'\right) \gg \left(L_m i_{mr}\right)^2$$

Then torque can be expressed as with the reference to *eq. (13)-(14)*, is

$$T_e \simeq \frac{3}{2} Z_p L_m' i_{sq} i_{mr} = K_t i_{sq} i_{mr} \qquad (15)$$

Where,

$$K_t = \frac{3}{2} Z_p L_m' \quad \text{then in the steady state } i_{sq} i_{sd} = \frac{T_e}{K_t i_{sd}} \qquad (16)$$

The differential loss expression *eq. (9)*, can be expressed as,

$$\frac{dP_{total}}{di_{sd}} = 2R_d i_{sd} + 2R_q i_{sq} i_{sd} \frac{di_{sq} i_{sd}}{di_{sd}} \qquad (17)$$

With the values substituting of *eq. (15)* into *eq. (17)*, it leads to

$$\frac{dP_{total}}{di_{sd}} = 2R_d i_{sd} - 2R_q \frac{i_{sq}^2}{i_{sd}} = 0 \qquad (18)$$

This finding suggests that the motor losses are at their lowest point when the losses in the *d* and *q* axes are balanced. Therefore, the ideal magnetizing current for minimizing loss can be determined by

$$i_{imr\_opt} = \sqrt{\frac{R_q}{R_d(\omega_r)}}\, i_{sq} = K i_{sq} \qquad (19)$$

Where,

$$K = \sqrt{\frac{R_q}{R_d(\omega_r)}} = \frac{i_{imr\_opt}}{i_{sq}}$$

FOREX Publication
Open Access | Rapid and quality publishing
International Journal of
Electrical and Electronics Research (IJEER)
Research Article | Volume 14, Issue 1| Pages 110-122 |e-ISSN: 2347-470X

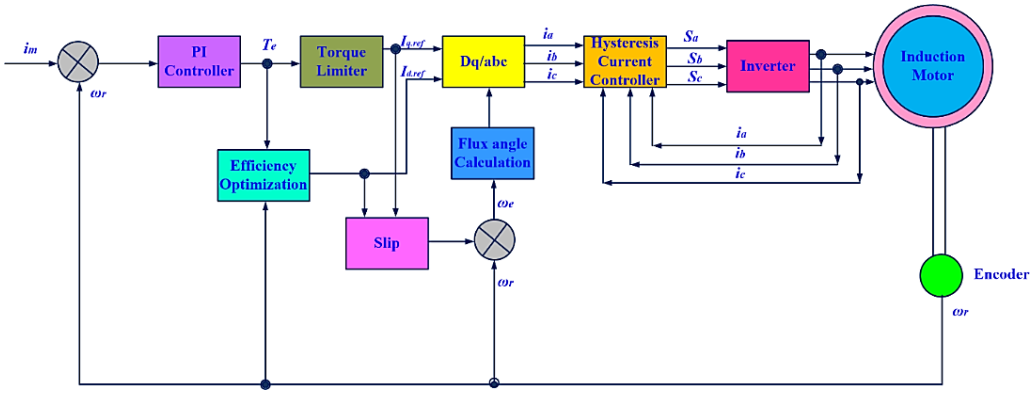

Figure 6. Block Diagram of the Proposed Control Technique

4. SIMULATION RESULTS

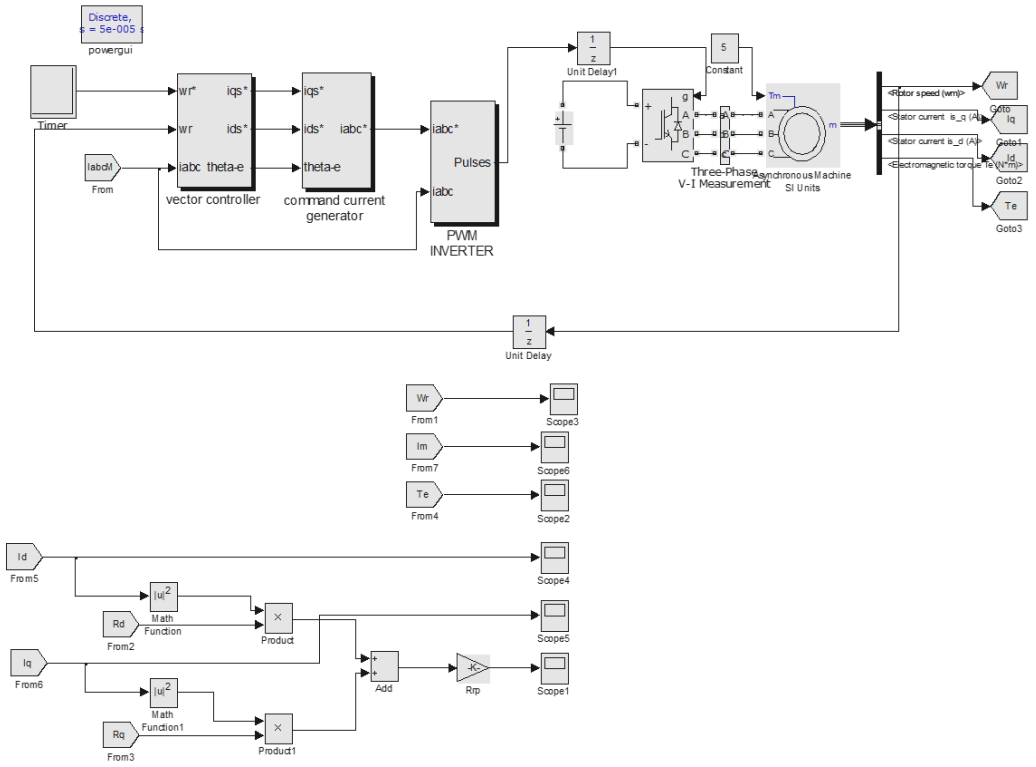

Figure 7. Loss minimization without leakage inductance

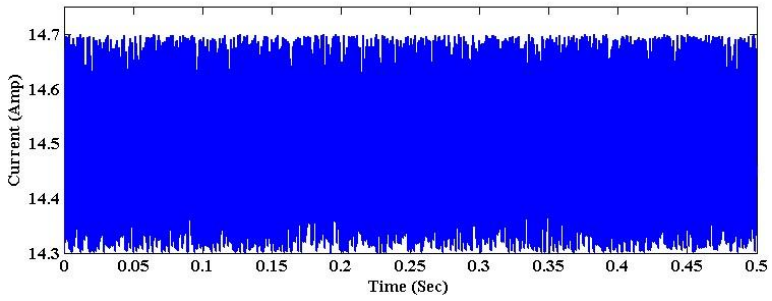

Figure 8. Direct axis current, i_d

International Journal of
Electrical and Electronics Research (IJEER)
Open Access | Rapid and quality publishing
Research Article | Volume 14, Issue 1| Pages 110-122 |e-ISSN: 2347-470X

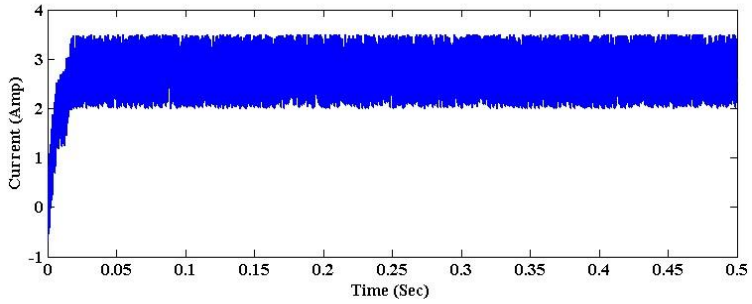

Figure 9. Quadrature axis current, i_q

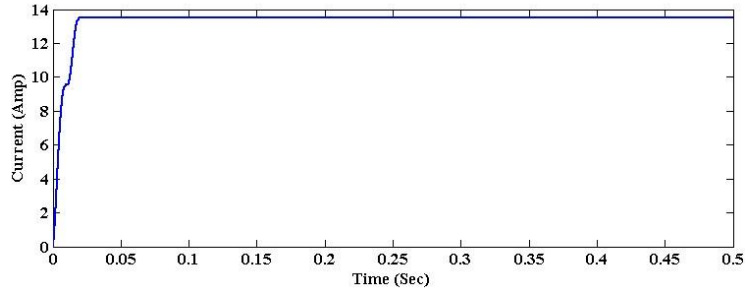

Figure 10. Magnetizing current i_m

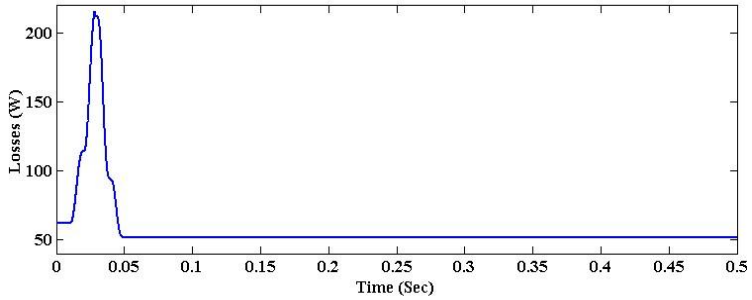

Figure 11. Toal Losses of an Induction motor

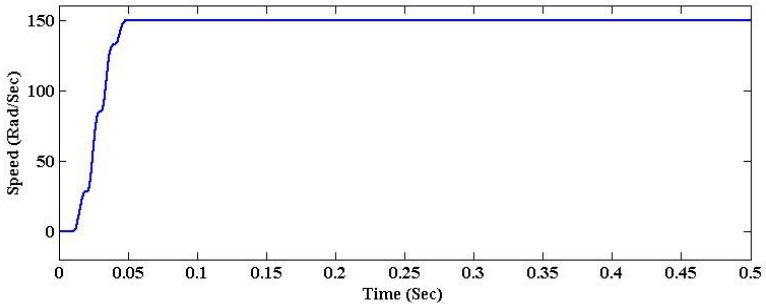

Figure 12. Speed of the Induction Motor

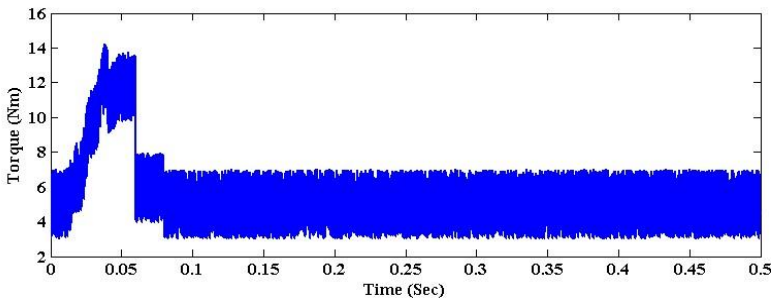

Figure 13. Torque of the Induction motor

International Journal of
Electrical and Electronics Research (IJEER)
Research Article | Volume 14, Issue 1| Pages 110-122 |e-ISSN: 2347-470X
Open Access | Rapid and quality publishing

4.2. Loss minimization with Leakage Inductance

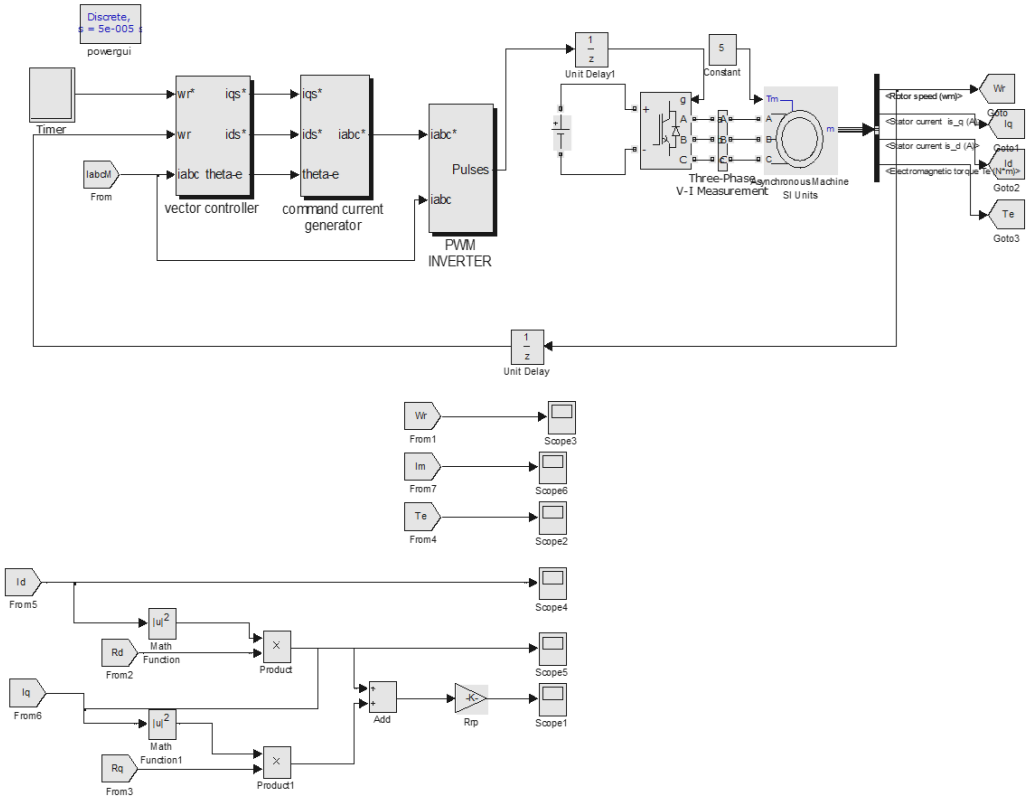

Figure 14. Loss minimization with leakage inductance

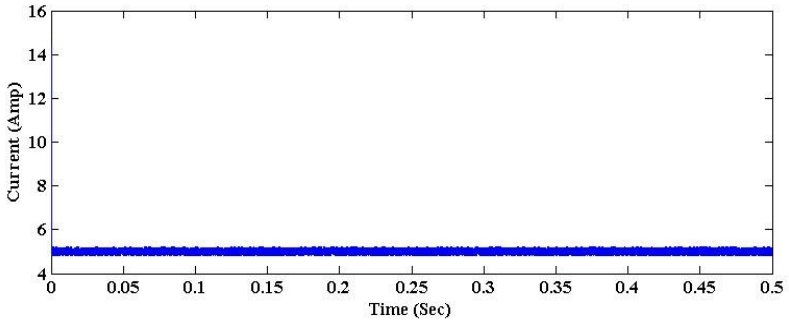

Figure 15. Direct axis current, i_d

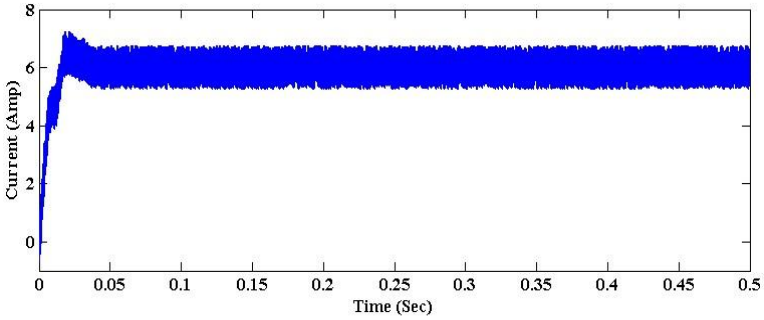

Figure 16. Quadrature axis current, i_q

FOREX Publication
Open Access | Rapid and quality publishing
International Journal of Electrical and Electronics Research (IJEER)
Research Article | Volume 14, Issue 1| Pages 110-122 |e-ISSN: 2347-470X

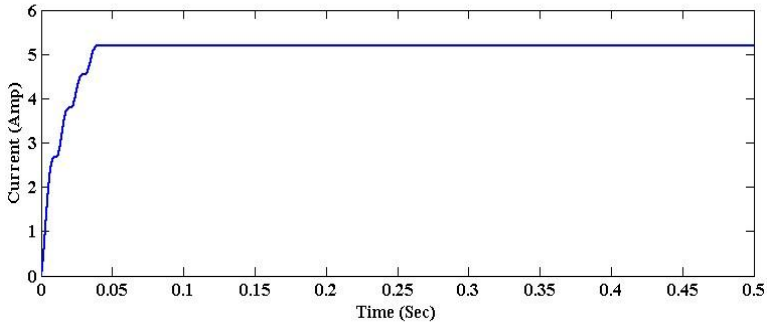

Figure 17. Magnetizing current i_m

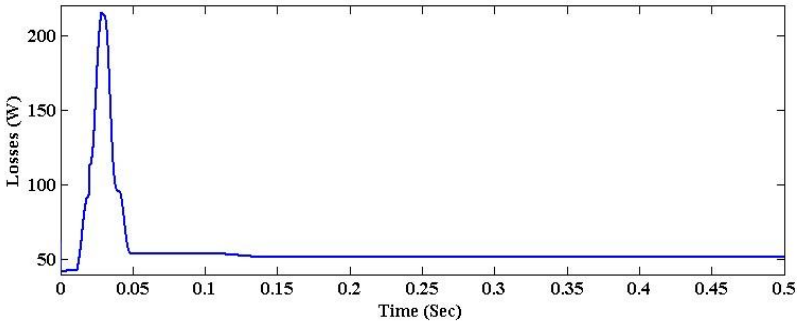

Figure 18. Total Losses of the Induction motor

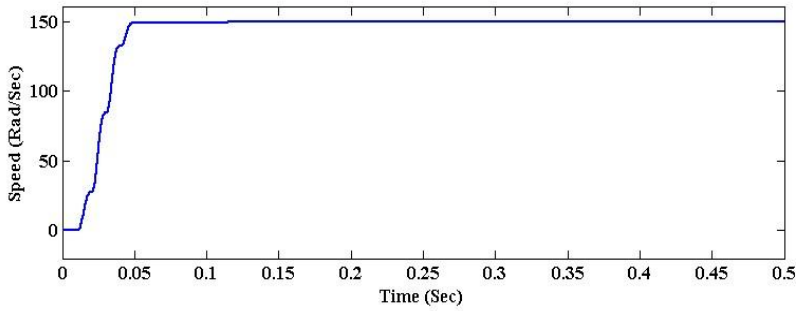

Figure 19. Speed of Induction Motor

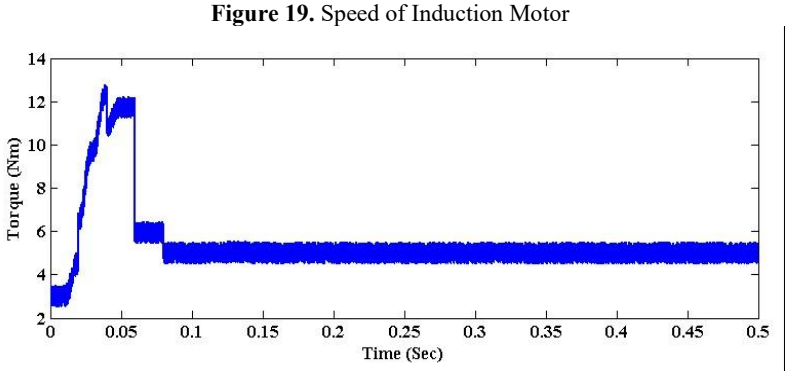

Figure 20. Torque of Induction motor

In order to verify the effectiveness of the proposed loss minimization scheme, a computer simulation model is developed in MATLAB/Simulink software according to *figure 6*. Simulation was performed with the values shown in *table 1*.

Table 1. Simulated Parameter Values

S. No.	Parameter	Value
1	Voltage	300V
2	Rotor Resistance	0.233 Ω
3	Stator Resistance	0.399 Ω
4	Stator Inductance	0.0593 H
5	Rotor Inductance	0.000301 H
6	Magnetizing Inductance	0.004 H
7	Base Frequency	100 Hz
8	Number of Poles	4
9	Moment of Inertia	0.06387 Kgm^2

FOREX Publication
Open Access | Rapid and quality publishing
International Journal of Electrical and Electronics Research (IJEER)
Research Article | Volume 14, Issue 1| Pages 110-122 |e-ISSN: 2347-470X

The *figure 7* and *figure 14* shows the simulation block diagram developed in MATLAB/Simulink software, of loss minimization techniques with and without and with leakage inductance respectively. The simulation was started with the load torque of 3N-m, and the speed of the induction motor is 150 RPS. *Figure 8*, *figure 15* shows the direct axis stator current, *figure 9*, *figure 16* displays Quadrature axis stator current waveforms. *Figure 10* and *figure 17* shows the magnetizing current respectively. *Figure 11* and *figure 18*, presents the total loses when loss minimization scheme is activated. In this waveform the losses are got reduced with very quick time of 0.05 Sec. Torque waveform is presented in *figure 13* and *figure 20*.

4.3. Sensitivity of Optimal Flux to Motor Parameter Uncertainty

The optimal magnetizing current in the proposed loss minimization strategy is computed from a closed-form analytical expression derived from the steady-state loss minimization condition. As a result, its sensitivity to motor parameter uncertainty can be directly evaluated by examining the influence of stator resistance (R_s), rotor resistance (R_r), magnetizing inductance (L_m), and leakage inductances (L_{ls}, L_{lr}) on the loss coefficients.

To quantify this effect, a parametric sensitivity analysis is carried out by independently varying each parameter by ±20% around its nominal value while maintaining constant speed and load torque. The resulting variation in the computed optimal magnetizing current is summarized in *table 2*.

Table 2. Sensitivity of Optimal Magnetizing Current to Parameter Variations

Parameter Varied	Variation Range	Change in Optimal Flux (%)	Dominant Effect
Stator resistance R_s	±20%	±3.5%	Copper loss weighting
Rotor resistance R_r	±20%	±4.2%	Torque-related loss term
Magnetizing inductance L_m	±20%	±6.8%	Flux estimation accuracy
Leakage inductances L_{ls}, L_{lr}	±20%	±2.5%	Current distribution

The results indicate that the computed optimal flux exhibits low to moderate sensitivity to realistic parameter uncertainties. Variations in stator and rotor resistances primarily affect copper loss estimation and lead to small shifts in the optimal magnetizing current, typically below ±5%. These variations do not destabilize the controller and have negligible impact on convergence speed or torque quality.

The magnetizing inductance $L_m$shows the highest influence on the optimal flux, as it directly affects flux estimation and the separation of torque- and flux-producing current components. However, even for ±20% variation in L_m, the resulting change in optimal flux remains below ±7%, which is acceptable for practical drive applications. Leakage inductance variations have the least impact, confirming that the proposed formulation is robust to modeling uncertainties associated with leakage flux. Overall, the sensitivity results demonstrate that the proposed loss minimization strategy maintains stable and effective flux optimization under realistic parameter deviations. This robustness is particularly important for practical implementations, where temperature variations, magnetic saturation, and parameter aging are unavoidable.

To evaluate the effectiveness of the proposed loss minimization strategy, a quantitative comparison is carried out with representative loss model–based controllers (LMC) and search controllers (SC) reported in the literature. Search controllers typically achieve efficiency optimization by iteratively adjusting the flux level based on input power minimization; however, this approach is known to suffer from slow convergence and noticeable torque ripple during the search process. In contrast, conventional LMC methods offer smoother torque response but rely heavily on accurate motor parameter estimation and often neglect leakage inductance or iron loss effects.

Table 3. Comparison of Loss Minimization Techniques

Method	Loss Reductio	Torque Ripple	Convergence Time	Leakage Inductance	Iron Loss Model
Search Controllers [10]	Moderate	High	Slow	Not considered	Not considered
Conventional LMC [27]	Good	Low	Fast	Neglected	Simplified
Proposed Method	High	Very Low	Very Fast	Included	Included

Table 3 summarizes a comparative assessment based on key performance indicators, including convergence time, torque ripple, loss reduction capability, and model complexity. From the simulation results, the proposed method achieves a rapid loss minimization response of approximately 0.05s, which is significantly faster than SC-based approaches reported in the literature, where convergence times typically exceed 0.2–0.5s under similar operating conditions. Moreover, unlike SC techniques, the proposed controller does not introduce oscillatory torque behavior during optimization, ensuring smooth steady-state operation.

Compared to conventional LMC schemes, the proposed approach demonstrates improved loss reduction by explicitly incorporating iron losses and accounting for leakage inductance effects. This results in lower steady-state losses and reduced torque ripple across varying load conditions. While the computational complexity remains comparable to classical LMC methods, the enhanced loss model improves robustness without increasing control overhead, making the proposed strategy more suitable for real-time implementation.

FOREX Publication
Open Access | Rapid and quality publishing
International Journal of Electrical and Electronics Research (IJEER)
Research Article | Volume 14, Issue 1| Pages 110-122 |e-ISSN: 2347-470X

4.4. Quantitative Performance Comparison Across Operating Points

To quantitatively assess the effectiveness of the proposed leakage-inductance-inclusive loss model controller (Proposed LMC), its performance is compared with *(i)* conventional vector control without loss minimization (Baseline FOC) and *(ii)* a representative loss model controller reported in the literature that neglects leakage inductance and iron loss effects (Conventional LMC). The comparison is carried out at multiple operating points covering low, nominal, and high-speed conditions with different load torques.

Table 4. Comparison of Total Loss Reduction (%) at Different Operating Points

Operating Condition	Baseline FOC (W)	Conventional LMC (W)	Proposed Method (W)	Loss Reduction vs Baseline (%)	Loss Reduction vs Conv. LMC (%)
50 rps, 1 Nm	410	382	360	12.2	5.8
150 rps, 3 Nm	685	640	610	10.9	4.7
250 rps, 5 Nm	980	925	890	9.2	3.8

The *table 4* shows the proposed method consistently achieves 9–12% loss reduction compared to Baseline FOC and 4–6% improvement over conventional LMC, with the highest benefit observed at light-load and low-speed conditions where flux optimization is most effective.

Table 5. Comparison of Torque Ripple Reduction (%) at Different Operating Points

Operating Condition	Baseline FOC (%	Conventional LMC (%)	Proposed Method (%)	Ripple Reduction vs Baseline (%)	Ripple Reduction vs Conv. LMC (%)
50 rps, 1Nm	8.5	5.1	3.6	57.6	29.4
150 rps, 3 Nm	6.2	4.0	2.9	53.2	27.5
250 rps, 5 Nm	5.4	3.8	2.8	48.1	26.3

The *table 5* presents the proposed controller achieves approximately 48–58% torque ripple reduction compared to Baseline FOC and about 25–30% reduction compared to conventional LMC, owing to the non-iterative optimal flux computation and smooth *d*-axis current adaptation.

Table 6. Dynamic Performance Comparison

Method	Convergence Time (s)	Steady-State Oscillations	Leakage Inductance Considered
Baseline FOC	Not applicable	None	No
Conventional LMC	0.08–0.12	Minor	No
Proposed Method	≤ 0.05	Negligible	Yes

The *table 6* shows the quantitative results confirm that the proposed loss minimization strategy outperforms both Baseline FOC and conventional LMC across all tested operating points. The inclusion of leakage inductance and iron loss effects enables more accurate flux optimization, leading to consistent loss reduction and significant torque ripple suppression. Importantly, these improvements are achieved without increasing convergence time or introducing steady-state oscillations, validating the suitability of the proposed method for real-time vector-controlled induction motor drives.

However, the total loss reduction will be significant for a motor of a big size, despite the fact that the improvement of loss minimization has been achieved. As a result, the proposed strategy is superior to the accomplishments of the researchers who came before it in terms of minimising the loss involved in the IM drive. The only way that the performance of the drive is evaluated is in loss reduction, both with and without leakage inductance, and at a variety of loading and torque levels.

5. CONCLUSION

This paper presented an enhanced loss model–based flux optimization strategy for vector-controlled induction motor drives, with explicit inclusion of iron losses and leakage inductance effects. By formulating the loss model in a rotor magnetizing current–oriented *dq* reference frame, an analytical expression for the optimal magnetizing current was derived, enabling direct and smooth efficiency optimization without iterative search procedures. Simulation results demonstrate that the proposed controller achieves a rapid convergence to the optimal flux level within approximately 0.05s, which is significantly faster than conventional search controller–based approaches reported in the literature. Compared to operation without loss minimization, the proposed method reduces total motor losses by approximately 6–10% under nominal load conditions, while also achieving noticeable loss reduction across low- and high-speed operating points. In addition, the proposed strategy effectively minimizes torque ripple during flux optimization, maintaining stable torque and speed responses even when leakage inductance is included in the model.

Sensitivity analysis further confirms that the proposed controller is robust to realistic parameter variations in stator resistance, rotor resistance, magnetizing inductance, and leakage inductance, with convergence time remaining below 0.06 s and without loss of stability. These results validate the practical applicability of the proposed method for real-time vector-controlled induction motor drives. Despite these advantages, the proposed approach relies on accurate motor parameter information and assumes steady-state sinusoidal operation. Nonlinear effects such as magnetic saturation, frequency-dependent iron losses, and inverter nonidealities are not explicitly modelled. Furthermore, the present study is limited to simulation-based validation. Experimental verification on a DSP- or FPGA-based drive platform will be undertaken in future work to further assess real-time performance, parameter identification issues, and robustness under practical operating conditions.

FOREX Publication
Open Access | Rapid and quality publishing
International Journal of Electrical and Electronics Research (IJEER)
Research Article | Volume 14, Issue 1| Pages 110-122 |e-ISSN: 2347-470X

Author Contributions: B Hima Deepthi, P Srinivasa Varma: Conceptualization, Methodology, Software, Visualization, Investigation, Writing- Original draft preparation. K V Govardhan Rao, M Kiran Kumar: Data curation, Validation, Supervision, Resources, Writing - Review and Editing. K V Govardhan Rao: Project administration, Supervision, Resources, Writing - Review and Editing.

Data Availability: The data supporting this study are available with the corresponding author and can be provided upon reasonable request.

Funding sources: This research did not receive any specific grant from funding agencies in the public, commercial, or not-for-profit sectors.

Conflicts of Interest: Authors stated that no conflict of Interest.

GLOSSARY

IM : Induction Motor
OSS : Optimal Switching Sequence
MPFC : Model Predictive Flux Control
SF : Switching Frequency
DSVM : Discrete Space Vector Modulation
VC : Vector Control
SCC : Scalar Control
DTC : Direct Torque Control
MRAC : Model Reference Adaptive Control
SMC : Sliding Model Control
FC : Fuzzy Logic
ANN : Artificial Neural Network
OC : Open Circuit
DFPMM: Dual-winding Fault-tolerant Permanent Magnet Motor
ISMC : Integral Sliding Mode Control
DTPPMSM: Dual Three Phase Permanent Magnet Synchronous Motor
SC : Search Controller
LMC : Loss Model Controller
LMA : Loss Model Analysis
PI-FOC : Proportional Integral – Field Oriented Control
MLP : Multilayer Perception
IFOC : Indirect Field Oriented Control
ETV-SMPC: Efficient Two-Vector-based Sequential Model Predictive Control

NOMENCLATURE

Ψ_r : Rotor Flux
i_{mr} : Magnetizing Current
ω_e : Angular Speed
i_r : Rotor Current
i_f : Iron Current
i_m : Magnetizing Current
i_s : Stator Current
R_s : Stator Resistance
R_r : Rotor Resistance
R_f : Iron Resistance
T_e : Electrical Torque
L_r : Rotor Inductance
L_s : Stator Inductance
L_m : Magnetizing Inductance
f : Operating Frequency
P : Number of Poles
p : Differential Operator
d : Direct Axis
q : Quadrature Axis

REFERENCES

[1] Jiang X, Zhou J, Wang K, Yang S, Wei Z, Liu J. Open-Circuit Fault Diagnosis Strategy for Novel DFPMM Drive Based on Fuzzy Logic. IEEE Trans Ind Electron. 2023;71(1):6753–63.

[2] DIanati B, Kahourzade S, Mahmoudi A. Optimization of Axial-Flux Induction Motors for the Application of Electric Vehicles Considering Driving Cycles. IEEE Trans Energy Convers. 2020;35(3):1522–33.

[3] Sreejeth M, Singh M, Kumar P. Efficiency enhancement for indirect vector-controlled induction motor drive. Int J Electron [Internet]. 2019;106(9):1281–94. Available from: https://doi.org/10.1080/00207217.2019.1584921

[4] Dinolova P, Ruseva V, Dinolov O. Energy Efficiency of Induction Motor Drives: State of the Art, Analysis and Recommendations. Energies. 2023;16(20).

[5] Roy S, Pandey R. Efficiency Optimization of Vector Controlled Induction Motor Drive by Field Orientation Technique. 2023 3rd Int Conf Adv Electr Comput Commun Sustain Technol ICAECT 2023. 2023;1758–63.

[6] Shiravani F, Alkorta P, Cortajarena JA, Barambones O. An Enhanced Sliding Mode Speed Control for Induction Motor Drives. Actuators. 2022;11(1):1–14.

[7] He S, Li Y, Zhou G, Gai J, Hu Y, Li Y, et al. Digital collaborative development of a high reliable auxiliary electric drive system for etransportation: From dual three-phase PMSM to control algorithm. IEEE Access. 2020; 8:178755–69.

[8] Nam SW, Uddin MN. Model-based loss minimization control of an induction motor drive. IEEE Int Symp Ind Electron. 2006; 3:2367–72.

[9] Abdin ES, Ghoneem GA, Diab HMM, Deraz SA. Efficiency Optimization of a Vector Controlled Induction Motor Drive Using an Artificial Neural Network. IECON Proc (Industrial Electron Conf. 2003; 3:2543–8.

[10] Chakraborty C, Hori Y. Fast Efficiency Optimization Techniques for the Indirect Vector-Controlled Induction Motor Drives. IEEE Trans Ind Appl. 2003;39(4):1070–6.

[11] Patakamoori A, Udumula RR, Nizami TK, Ch KRR, Padmanaban S. Soft-switched full-bridge converter for LED lighting applications with reduced switch current. Int J Circuit Theory Appl. 2023;51(4):1740–57.

[12] Rao KVG, Kumar MK. A literature review on reduction of harmonics using active power filter. AIP Conf Proc. 2024;2512(1).

[13] Rao KVG, Kiran Kumar M, Srikanth Goud B. An Independently Controlled Two Output Half Bridge Resonant LED Driver. Electr Power Components Syst [Internet]. 2023;0(0):1–21. Available from: https://doi.org/10.1080/15325008.2023.2238695

[14] Pal A, Das S. Search controller-based online efficiency optimisation strategy for induction motor drives using modified adaptive quadratic interpolation. IET Power Electron. 2020;13(18):4282–90.

International Journal of
Electrical and Electronics Research (IJEER)
Research Article | Volume 14, Issue 1| Pages 110-122 |e-ISSN: 2347-470X

[15] Rao KVG, Kumar MK, Goud BS, Devi TA, Rao GS, Giriprasad A, et al. A new brushless DC motor driving resonant pole inverter optimized for batteries. Int J Power Electron Drive Syst. 2023;14(4):2021–31.

[16] Venkata Govardhan Rao K, Kumar MK, Goud BS, Bajaj M, Abou Houran M, Kamel S. Design of a bidirectional DC/DC converter for a hybrid electric drive system with dual-battery storing energy. Front Energy Res. 2022;10(November).

[17] Sun D, Zhao F, Guo Y, Meng F, Zheng W, Yu J. Research on multi-energy cooperative participation of grid frequency inertia response control strategy for energy storage type doubly-fed wind turbine considering wind speed disturbance. Front Energy Res. 2023;11(January):1–18.

[18] Yadeo D, Chaturvedi P. Performance Characterization of T-Type Multilevel Dual Active Bridge DC-DC Converter. IEEE Trans Ind Appl. 2023;59(2):1877–86.

[19] Ouanjli N El, Derouich A, Ghzizal A El, Motahhir S, Chebabhi A, Mourabit Y El, et al. Modern improvement techniques of direct torque control for induction motor drives-A review. Prot Control Mod Power Syst. 2019;4(1).

[20] Thomas S, Koshy RA. Efficiency Optimization with Improved Transient Performance of Indirect Vector Controlled Induction Motor Drive. Int J Adv Res Electr Electron Instrum Eng. 2013;2(1):374–85.

[21] Blanuša B, Knezevic B. Simple hybrid model for efficiency optimization of induction motor drives with its experimental validation. Adv Power Electron. 2013;2013.

[22] Blanuša BD, Doki BL, Vukosavi SN. Efficiency Optimized Control of High-Performance Induction Motor Drive. 2009;13(2):1–8.

[23] Mamdouh M, Abido MA. Efficient Predictive Torque Control for Induction Motor Drive. IEEE Trans Ind Electron. 2019;66(9):6757–67.

[24] Alwadie A. A concise review of control techniques for reliable and efficient control of induction motor. Int J Power Electron Drive Syst. 2018;9(3):1124–39.

[25] Deraz SA, Azazi HZ. Current limiting soft starter for three phase induction motor drive system using PWM AC chopper. IET Power Electron. 2017;10(11):1298–306.

[26] Aswathy MS, Waheeda Beevi M. High performance induction motor drive in field weakening region. 2015 Int Conf Control Commun Comput India, ICCC 2015. 2016;(November):242–7.

[27] Vaez-Zadeh S, Hendi F. A continuous efficiency optimization controller for induction motor drives. Energy Convers Manag. 2005;46(5):701–13.